Noname manuscript No.
(will be inserted by the editor)

A Model for the Neuronal Substrate of Dead Reckoning and Memory in Arthropods: A Comparative computational and Behavioral Study.

Ulysses Bernardet · Sergi Bermúdez i Badia · Paul FMJ Verschure

the date of receipt and acceptance should be inserted later

Abstract Returning to the point of departure after exploring the environment is a key capability for most animals. In the absence of landmarks, this task will be solved by integrating direction and distance traveled over time. This is referred to as path integration or dead reckoning. An important question is how the nervous systems of navigating animals such as the $1mm^3$ brain of ants can integrate local information in order to make global decision. In this article we propose a neurobiologically plausible system of storing and retrieving direction and distance information. The path memory of our model builds on the well established concept of population codes, moreover our system does not rely on trigonometric functions or other complex non-linear operations such as multiplication, but only uses biologically plausible operations such as integration and thresholding. We test our model in two paradigms; in the first paradigm the system receives input from a simulated compass, in the second paradigm, the model is tested against behavioral data recorded from 17 ants. We were able to show that our path memory system was able to reliably encode and compute the angle of the vector pointing to the start location, and that the system stores the total length of

Ulysses Bernardet
Synthetic Perceptive, Emotive and Cognitive Systems (SPECS)
Universitat Pompeu Fabra
Tànger, 135
E-08018 Barcelona, Spain
Tel: (+34) 93-542-1545
E-mail: ubernardet@iua.upf.edu

Sergi Bermúdez i Badia
SPECS, Technology Department
Universitat Pompeu Fabra
Tànger, 135
E-08018 Barcelona, Spain
E-mail: sergi.bermudez@upf.edu

Paul FMJ Verschure
ICREA, SPECS, Technology Department
Universitat Pompeu Fabra
Tànger, 135
E-08018 Barcelona, Spain
E-mail: paul.verschure@iua.upf.edu

the trajectory in a dependable way. From the structure and behavior of our model, we derive testable predictions both at the level of observable behavior as well as on the anatomy and physiology of its underlying neuronal substrate.

Keywords path integration; dead reckoning; arthropod; path memory; population code; vector decoding; neuronal model

1 Introduction

Relocating the nest after leaving the dwelling and moving about in the environment is a basic requirement for any entity living in the real-world, a task which needs to be solved by human and bug. Two strategies can be used to find the way back to the point of departure: Firstly, the agent can memorize its path based on external cues such as visual, auditory, or olfactory landmarks, or secondly, the agent can integrate the distance and direction traveled. Commonly, the former is referred to as "landmark navigation" (LMN), and the latter is called "path integration" (PI) or "dead reckoning" (figure 1). Dead reckoning is thought to have been introduced into the scientific discourse in the 19^{th} century by Darwin [4].

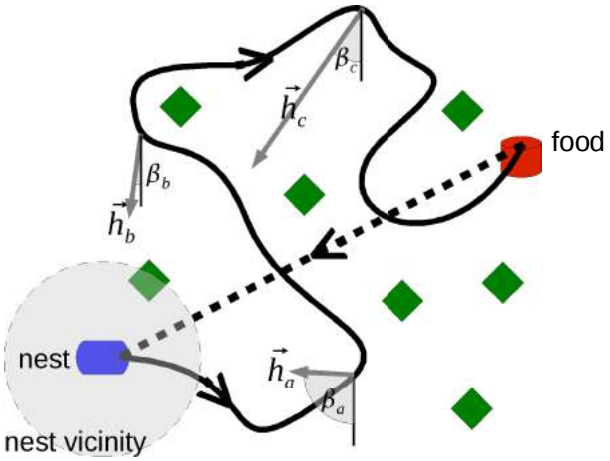

Figure 1 An Example of path integration based navigation. The outbound journey is marked with a solid line, and the return path with a dashed line. Diamonds mark the location of landmarks. $\overrightarrow{h_a}$, $\overrightarrow{h_b}$, $\overrightarrow{h_c}$ indicate vectors pointing to the departure location, β_a, β_a, β_a indicate the corresponding angles of the home-wards pointing vectors.

Path integration has been studied extensively in insects (for review: [55]) as well as in mammals (for review: [8]). Experimental research on path integration in insects has been pioneered by the work of von Frisch [50] on bees and of Wehner [54] on ants. Von Frisch, for example, could show already in the 1960s that bees signal by ways of their waggle-dance the air-line direction to a nectar source, irrespective of whether they had to fly a detour to actually get there or not [50]. The empirical verification of vertebrate path integration strategies has been put forward more recently [31].

To integrate the path, two signals are required; the traveling direction and the traveling distance. While the sources of information for path integration in insects are

well investigated, it is presently not clear which of several possible cues mammals are making use of, e.g. vestibular information, proprioceptive information, sensory flow, or efferent copies from movement commands [52].

1.1 Measuring the traveled distance

Walking insects like ants have been shown to predominantly use proprioception to estimate the distance traveled during a journey [38,58,42,56]. In flying insects, the consumption of energy was thought to be used as a means to measure distance. This is referred to as the "energy hypothesis" [50]. Yet research has shown that this hypothesis cannot be upheld (reviewed in [7]). Bees have been shown in both, laboratory [44,41, 17] and natural settings [47], to rely on optic flow to gauge distance.

1.2 Measuring the heading direction

A large variety of terrestial and aquatic animals are using the so called "solar compass" for navigation. The solar compass derives heading information from the polarization pattern of the sky and possibly the luminance distribution of the sunlight. In the class of insects this has been shown for the desert ant (*Cataglyphis*: [53]), the cricket (*Gryllus campestris*: [20]), the locust (*Schistocerca gregaria*: [16]), the honeybee (*Apis mellifera*: [50,39]), the cockchafer beetle (*Melolontha melolontha*: [21]), the cockroach (*Leucophaea maderae*: [26]), the fly (*Musca domestica*: [51]) and the monarch butterflies (*Danaus plexippus*: [37,45]). At the behavioral level, ants have been studied most extensively, whereas in the domain of physiology, the best investigated animals are crickets and locusts.

The solar compass fulfills functions similar to the so called head direction cells (HDCs) found in mammals [19]. These head direction cells show an increase in firing rate that is specific to the animal's orientation, but not to the location in space and can be found in various brain areas, e.g. in the rat including but not limited to the postsubiculum, anterior dorsal nucleus of the anterior thalamus, and lateral mammillary nucleus [46].

1.3 Path memory models

Research on the memory of bees is predominantly phenomenological, and has shown that the working memory of bees is plastic and robust and is organized to work at different temporal scales [29,36,63]. Looking for the underlying mechanism, we have to turn to research on the fruit fly. In the *Drosophila*, neuronal structures for memory are showing a high degree of domain specificity, i.e. there is no central all-purpose memory structure. The mushroom bodies are the location of odor related short- [61] and long-term memories [34]. Visual memory traces can be found in the central complex, a neuronal structure with repetitive and regular organization [25]. The role of the median bundle is not entirely clear. Recent investigations are flagging it as a candidate for a kind of place memory, as it is the integration site for sensory information e.g. from the antennae, and path information from the ventral ganglion [62]. Hence, although

the actual location of the path integrator and memory has not yet been identified, the ventral ganglion seems to be a good candidate [62].

Many of the above mentioned mechanisms are in the realms of long-term memory, and would seem to require synaptic changes. The question is, what the mechanisms of working and short-term memory are that could support path integration and dead reckoning. Here we will investigate two scenarios on such a memory system that is based on a population coding of heading direction. The standard way of calculating the homing vector is the linear summation of all memorized vectors. This procedure heavily relies on multiplicative and trigonometric operations. Though some are arguing that multiplicative operations are occurring in nervous systems [11] this issues is still under active investigation. A nervous system performing trigonometric operations, possibly relying on some kind of look-up table, seems highly improbable.

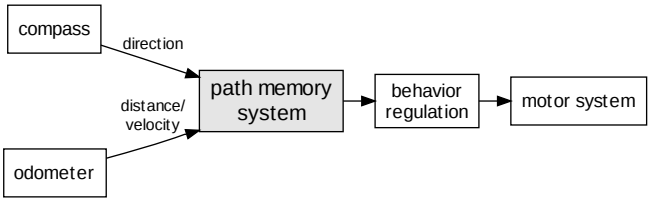

Figure 2 Diagram of the embedding of the path memory in a model of a foraging agent. The computation of the heading direction is provided by e.g. a solar compass system, whereas the distance information can stem e.g. from the optic flow, or proprioceptive information. Both signals are fed into the path memory system which in turn provides the behavior regulation system with the homing vector.

The memory subsystem of our model builds up on two concepts; neurons exhibiting persistent activity and the population code.

The persistent activity of tonically firing neurons is triggered by a short excitatory and shunted by a brief inhibitory input. Neurons showing these properties can be found in a wide variety of neuronal systems in a number of species that have also been associated with spatial navigation ([27] for review). Examples include the entorhinal cortex of rats [5], cultured Retzius cells of the leech [1], respiratory and flight system inter- and motoneurones in the locust [35], and cells in the antenna lobe of the moth [30].

The concept of a "population code" was pioneered by Georgopoulos' work on the motor cortex [13,12]. Systems employing this mechanism can be found in a wide range of biological neuronal systems [40], including the cricket's cercal sensory system [18]. The driving idea of the population code is the representation of a single vector as the sum of multiple vectors. Each of the single vectors is in turn represented by neurons. The angle of the vector is given by the direction dependent tuning curve of the neuron, whereas the length of the vector is represented by the spiking frequency. Hence in a vector population each neuron can be understood as vector $\overrightarrow{v}$ with norm $\|v\|$ proportional to the firing rate and an angle α given by the neuron's preferred direction (figure 3).

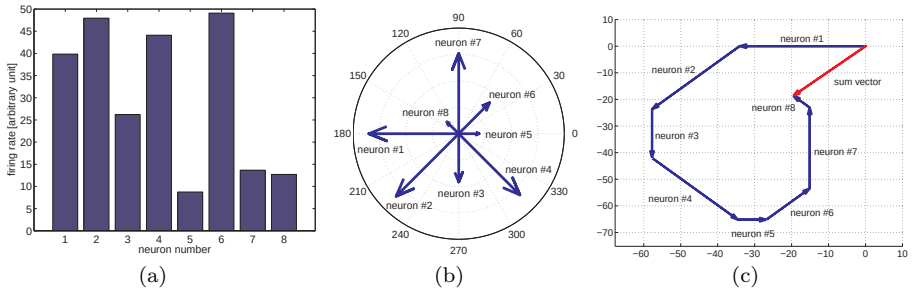

Figure 3 Illustration of the population code concept. (a) A group of cells – 8 in this case – can be understood as vector field, where each cell in the group represents a vector $\overrightarrow{v}$ with norm $\|v\|$ proportional to the firing rate and an angle α given by the neuron's preferred direction (b). (c) The sum vector $\overrightarrow{s}$ of all vectors $\overrightarrow{v}$ is indicated by a red arrow.

2 Methods

2.1 Path memory model

Our path memory model consists of three main stages: Input, memory, and memory decoding (figure 4). Subsequently we will elaborate the function and implementation of these different stages. For ease of explanation we will start with the memory storage mechanism before explaining the input to the memory.

Memory storage mechanism

The task of the memory is to store the direction and the distance traveled. In the *"Memory"* group, every neuron is associate with a specific direction. Each neuron has a narrow tuning curve of 10°. Neurons with the same preferred direction are organized into columns within the group (figure 5). This is not a conceptual requirement, but is useful to make the handling easier.

The neuron type used are of the type "Integrate and Fire" with a high membrane persistence. This means, that a single excitatory input spike to this cell suffices to trigger a sustained firing, whereas a single inhibitory input spike will pull the neuron back to the resting state. The persistent firing of the cells in the *"Memory"* group constitutes the mid-term memory mechanism. The schema of persistent firing is consistent with neurobiological findings in a wide range of neuronal systems [27]. Binary neurons are used in order make the system immune to possible fluctuations of the spiking frequency of a single neuron, and to increase the redundancy. In principle the system could also be implemented using neurons exhibiting graded persistent activity [5], which would increase the memory capacity, but make the memory more susceptible to the fluctuation of activity of single neurons.

In total the *"Memory"* group consists of 3600 neurons, organized into 36 columns. The length of the vectors pointing in the 36 different directions can be visualized by summing up the activity of all neurons in one column.

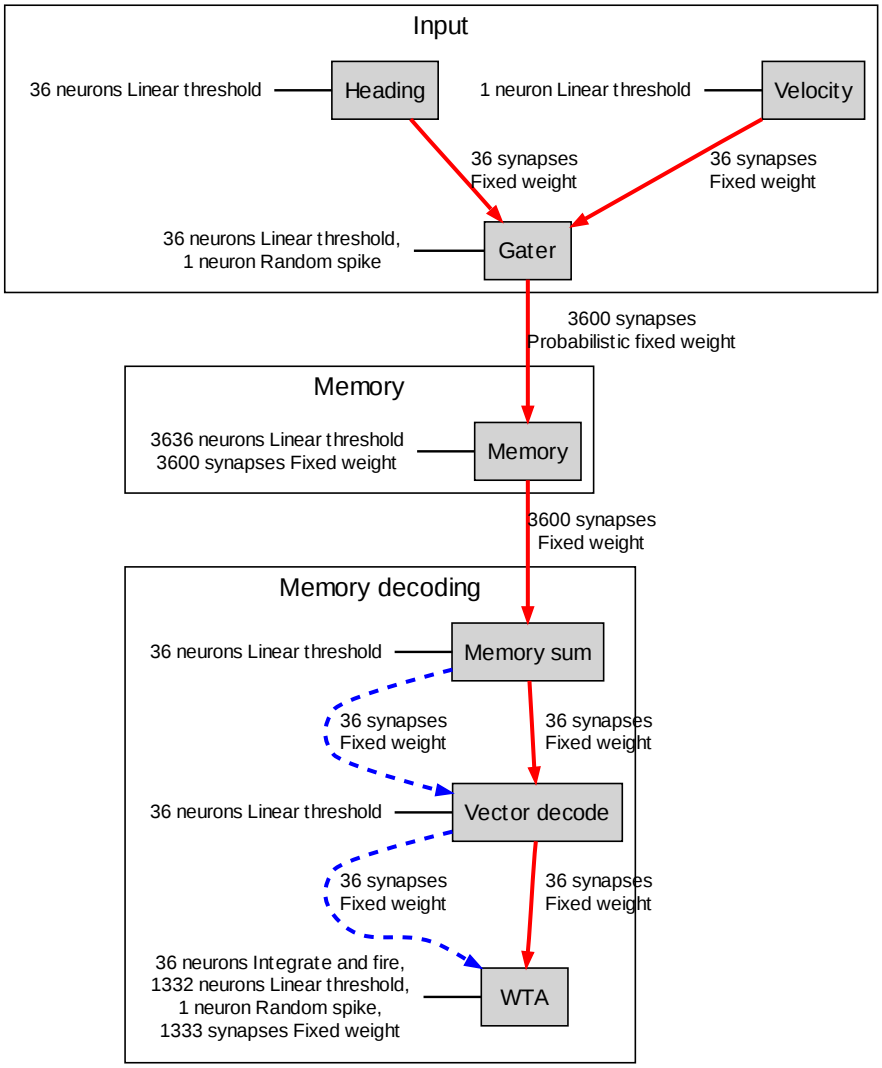

Figure 4 Architecture of the path memory model. Gray boxes stand for sub-systems. A sub-system can consist of a single cell group, or of multiple, connected groups. Excitatory connections are symbolized by solid red, inhibitory connections by dashed blue arrows. The *"Velocity"* group provides the velocity input from the odometry subsystem. In the *"Gater"* group the velocity input is combined with the heading direction. *"Memory"* is the main memory group organized into 36 columns of 100 neurons. Each neuron in one column of the *"Memory"* group projects onto the *"Memory sum"* group (36 neurons). Hence each neuron in the *"Memory sum"* group has an activity proportional to the number of active neurons in a column of the *"Memory"* group. Each neuron in the *"Memory sum"* represents a vector $\overrightarrow{v}$ with norm $\|v\|$ proportional to the firing rate and an angle α corresponding to the angle of a column of the *"Memory"* group (figure 5).

Input to the memory system

The heading direction information is provided via a *"Gater"* group (figure 4). In this group, only one cell is active at any given time, and its identity determines the agent's

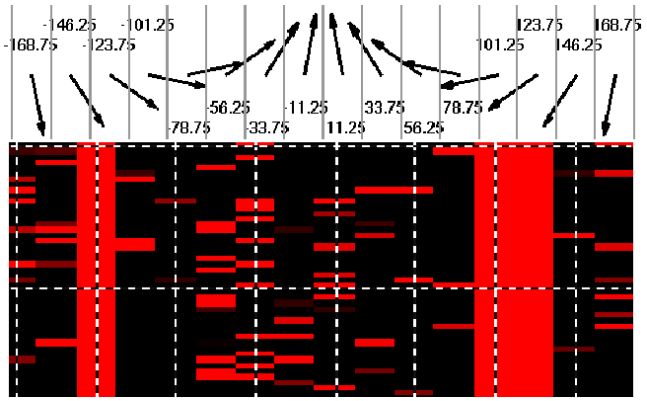

Figure 5 The basic concept of the path memory is the representation of the distance traveled in different directions by a population code. Each column in the *"Memory"* group (reddish columns at the bottom) represents a vector $\overrightarrow{v}$ in a direction j. Red stripes in the columns indicate tonically firing neurons, whereas in the black parts no neurons are active. The length of the vector component is given by the number of spiking neurons within a column. For illustration the figure shows a memory for 16 directions, as opposed to 36 direction used in the model.

heading direction (figure 6). The velocity information is provided by the odometry subsystem and is represented by the spiking frequency of the active cell in the *"Gater"* group. The activity of this group is linearly dependent on the traveling velocity.

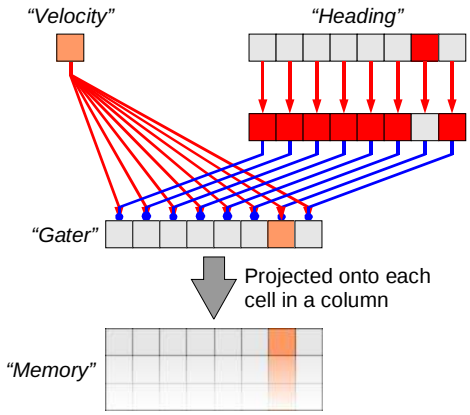

Figure 6 Illustration of the memory system input mechanism. The speed information represented by the group "*Velocity*" is projected onto each cell of the "*Gater*" group, but only the cell representing the current heading direction ("*Heading*") is active, all other cells are inhibited. For illustration the figure the input mechanism 8 directions, as opposed to 36 direction used in the model.

All cells within one column of the *"Memory"* group receive excitatory input from the corresponding cell in the *"Gater"* group, hence the position of the active cell in the *"Gater"* group defines which column within the memory group is activated.

The synapses between the *"Gater"* and the *"Memory"* groups are of type "probabilistic fixed weight". This probabilistic synapse type transfers the synaptic input $synIn$ to the post-synaptic potential psp with transmission probability $Prob$ and the synaptic weight $w \in [-1, 1]$ (equation 1).

$$psp_i(t+1) = \begin{cases} synIn_i(t) * w & \text{with probability } Prob \\ 0 & \text{otherwise} \end{cases} \quad (1)$$

The transmission probability for the synapses between the *"Gater"* and the *"Memory"* group is relatively small (0.05) therefore each excitatory/inhibitory pre-synaptic spike will only "kick" a relatively small number of post-synaptic cells above threshold. This probabilistic mechanism represents a sub-sampling of the actual heading direction input. Taken together, the number of currently spiking neurons in a column of the *"Memory"* group is proportional to the total distance traveled in a specific direction.

Memory readout mechanism

Having the path stored in memory is only useful, if we can subsequently retrieve this information. The goal of the memory readout is therefore to calculate the sum vector $\overrightarrow{s}$: $\overrightarrow{s} = \sum_{1 \le i \le n} \overrightarrow{v}_i$. For ease of illustration, we add a group *"Memory sum"* where each cell receives input from all cells of one columns of the *"Memory"* group (figure 4). Hence each neuron in the *"Memory sum"* has an activity proportional to the number of active neurons in a column of the *"Memory"* group, and represents a vector $\overrightarrow{v}$ with norm $\|v\|$ proportional to the firing rate and an angle α corresponding to the angle of a column of the *"Memory"* group. This intermediate step is not a requirement, but helps in constructing the system.

The solution we employ to approximate $\overrightarrow{s}$ is a two step process. In a first operation we project the vectors $\overrightarrow{v}_j$ represented by the neurons in the group *"Memory sum"* onto a set of projection neurons $\overrightarrow{p}_j$ (figure 7).

Secondly we apply a MAX operation in this population of projection neurons.

The first operation has been shown to theoretically yield a close approximation of the sum vector, while being biologically plausible and able to cope with a wide range of input tuning curves [40]. Indeed populations of neurons exhibiting response characteristics in accordance with this concept have been found in the form of interneurons in the motor system of the leech [24]. The number of $\overrightarrow{p}_j$ neurons is arbitrary, and determines the angular resolution of the sum vector $\overrightarrow{s}$ computation; the larger j, the more accurate the computation of $\overrightarrow{s}$ will be.

The **first** step, the computation of the projection vectors $\overrightarrow{p}_j$, is performed according to equation 2 and equation 3.

$$\|\overrightarrow{p}_j\| = \sum_{1 \le i \le n} \|\overrightarrow{v}_i\| \cdot w_{j-i} \quad (2)$$

$$w_{j-i} = cos(\Delta\alpha_{j-i}) \quad (3)$$

where $\Delta\alpha_{j-i} = [-180 \dots 180]$ is the angular difference between vector $\overrightarrow{p}_j$ and vector $\overrightarrow{v}_i$. The weight w_{j-i} is defined as a function of $\Delta\alpha_{j-i}$.

This operation is equivalent to a convolution operation between $\overrightarrow{v}$ and a cosine kernel equation 4.

$$\|\overrightarrow{p}_j\| = \|\overrightarrow{v}_i\| * w_i = \sum_{1 \leq i \leq n} \|\overrightarrow{v}_i\| \cdot w_{j-i} \tag{4}$$

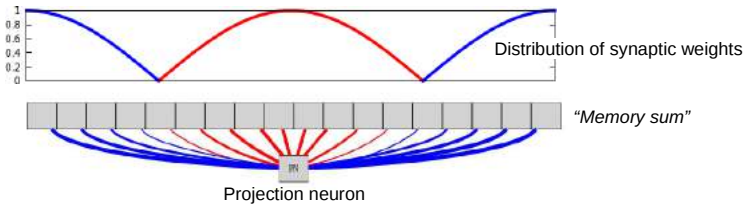

Figure 7 Illustration of the memory readout mechanism. The figure shows a single projection neuron, which receives input from the *"Memory sum"* group. Excitatory connections are symbolized by red, inhibitory connections by blue arrows. The synaptic weights are distributed in a Gaussian fashion, approximating a cosine distribution. The top panel shown the weight of the excitatory and inhibitory connection. In the bottom panel the weight of the connection is represented by the width of the connection. In total the "*Vector decode*" group (figure 4) consists of 36 projection neurons.

Since a cosine distribution of synaptic weight is biologically not very plausible, approximate the cosine distribution with a Gaussian function (figure 8).

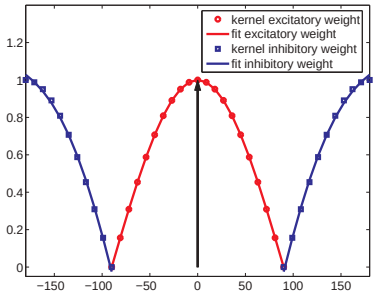

Figure 8 The cosine functions that define the synaptic weight are approximated with Gaussian functions with a mean square error (MSE) of .5217.

The **second** step of the approximation of the sum vector $\overrightarrow{s}$ is to apply a MAX operation on the projected vectors $\overrightarrow{p}$ (figure 4, "*WTA*"). Hence, $max(\|\overrightarrow{p_j}\|)$ represents the closest $\overrightarrow{p_j}$ vector to the sum vector $\overrightarrow{s}$.

The equivalent to a MAX operation is known as a Winner-Takes-All (WTA) network in biological systems. WTA networks are widely used in computational neural models, artificial neural networks and analog Very Large Scale Integration (aVLSI) circuits. These networks are used in associative memory models [15] where stored memories compete to explain input data, in cooperative models of binocular stereo [28], in biological models [6,9,59,60]), and in Fukushima's neocognitron [10]. In our model, a WTA network is used as the last step of the readout mechanism. The WTA network is used to locate the $\overrightarrow{s}$ displaying the highest activity, corresponding to the closest orientation to the actual sum vector of the memory content.

Table 1 Statistics of the number of elements (neurons, synapses) used in the path memory model for turn table and tracked ants experiments.

element type	count
Neurons	5151
Number of groups with neuron	
Integrate and Fire	1
Linear Threshold	11
Random Spike	2
Synapses	5187
Synapse types used	
Fixed Weight	14
Fixed Weight Probabilistic	2
Modules	0

2.2 Tracking system

The behavioral data was acquired with the custom-built general purpose video tracking suit called "AnTS" developed by the authors. The AnTS suit consists of three tools: A calibration tool, the core tracking application and an analysis tool (figure 9a). The core of the suit, the image processing component, builds on the Open Source Computer Vision Library (Intel, USA, San Jose). For the graphical user interface, the widget-set Qt is used (Trolltech, Norway). The AnTS tracking application produces one trace per tracked element, including its coordinates, time and whether the object was lost during tracking. In the setup described in this article, the AnTS tracking system received input from a CCD camera (Sony EVI-D31) at VGA resolution (640x480 pixel). The camera was fixed centrally ∼2m above the arena of the ants.

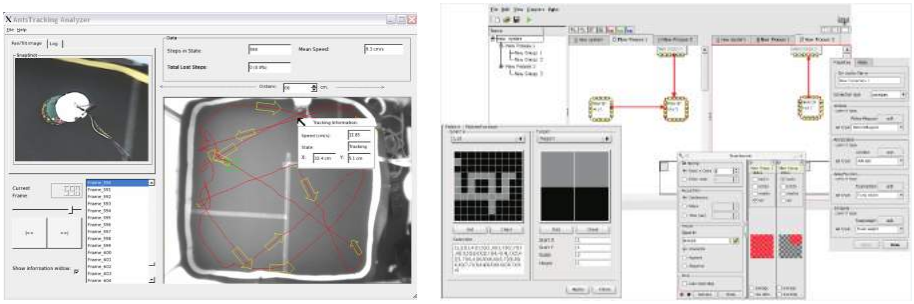

(a) (b)

Figure 9 a) Screen shot of the analysis tool of the "AnTS" tracking suit. The tool allows to analyze the traces generated by the AnTS tracking software, providing basic statistics of the data. b) Screen shot of the graphical user interface of the large-scale neural systems simulator `iqr`.

2.3 Simulation environment

All simulations were conducted with the large-scale neuronal systems simulator `iqr` developed by the authors [3]. `iqr` allows to graphically design and control neuronal

models (figure 9b), and to interface these systems to real-world devices. The key feature of `iqr` are: Graphical on-line control of the simulation, change of model parameters at run-time, on-line visualization and analysis of data, connect neural models to real-world devices (cameras, mobile robots, etc.), pre-defined neuron and synapse types, open architecture for new neurons, synapses, and hardware interfaces. `iqr` is implemented in C++ using the Qt widget-set (Trolltech, Norway, Oslo), and runs on the Linux and Apple's Mac OS X platform. The software comes fully documented, including a tutorial and an introduction on how to write user-specific extension, and is freely available as open-source software [2].

Subsequently we give the mathematical description of the neuron types used in our path memory model.

Linear threshold neuron Graded potential neurons are modeled using linear threshold cells. The membrane potential of a linear threshold cell i at time $t+1$, $v_i(t+1)$, is given by

$$\begin{aligned} v_i(t+1) = VmPrs_i v_i(t) \\ + ExcGain_i \sum_{j=1}^{m} w_{ij} a_j(t-\delta_{ij}) \\ - InhGain_i \sum_{k=1}^{n} w_{ik} a_k(t-\delta_{ik}) \end{aligned} \tag{5}$$

where $VmPrs_i \in \{0,1\}$ is the persistence of the membrane potential, $ExcGain_i$ and $InhGain_i$ are the gains of the excitatory and inhibitory inputs respectively, m is the number of excitatory inputs, n is the number of inhibitory inputs, w_{ij} and w_{ik} are the strengths of the synaptic connections between cells i and j and i and k respectively, a_j and a_k are the output activities of cells j and k respectively, and $\delta_{ij} \geq 0$ and $\delta_{ik} \geq 0$ are the delays of the projection from cell j to i and k to i respectively.

The output activity of cell i at time $t+1$, $a_i(t+1)$, is given by

$$a_i(t+1) = \begin{cases} v_i(t+1) \text{ with probability } Prob \text{ for } v_i(t+1) \geq ThSet \\ 0 \qquad\qquad \text{otherwise} \end{cases} \tag{6}$$

where $ThSet$ is the membrane potential threshold, and $Prob$ is the probability of activity.

Integrate and fire neuron Spiking cells are modeled with an integrate-and-fire cell model. The membrane potential is calculated using equation (5). The output activity of the cell at time $t+1$, $a_i(t+1)$ is given by

$$a_i(t+1) = \begin{cases} SpikeAmpl \text{ with probability } Prob \text{ for } v_i(t+1) \geq ThSet \\ 0 \qquad\qquad\quad \text{otherwise} \end{cases} \tag{7}$$

where $SpikeAmpl$ is the height of the output spikes, $ThSet$ is the membrane potential threshold, and $Prob$ is the spike probability.

After cell i produces a spike, the membrane potential is hyperpolarized such that

$$v_i^{'}(t+1) = v_i(t+1) - VmReset \tag{8}$$

where $v_i^{'}(t+1)$ is the membrane potential after hyperpolarization and $VmReset$ is the amplitude of the hyperpolarization.

Random spike neuron A random spike cell releases a spike per timestep with a user-defined spike probability. The time series of the output spikes forms a Poisson process. Unlike the other cell types, it receives no input and has no membrane potential. The output of a random spike cell i at time $t+1$, $a_i(t+1)$, is given by

$$a_i(t+1) = \begin{cases} SpikeAmpl & \text{with probability } Prob \\ 0 & \text{otherwise} \end{cases} \tag{9}$$

2.4 Performance measurements

The performance of the path memory system was evaluated using two paradigms. In the first paradigm, the path memory model was fed with simulated compass information, which corresponded to the model being placed on a continuously rotating turn table. The velocity input was set to a constant value.

In the second paradigm, behavioral data of ants (*Formica cunicularia*) exploring an arena was obtained using the general purpose visual tracking system tracking system "AnTS".

3 Results

3.1 Turn table experiments

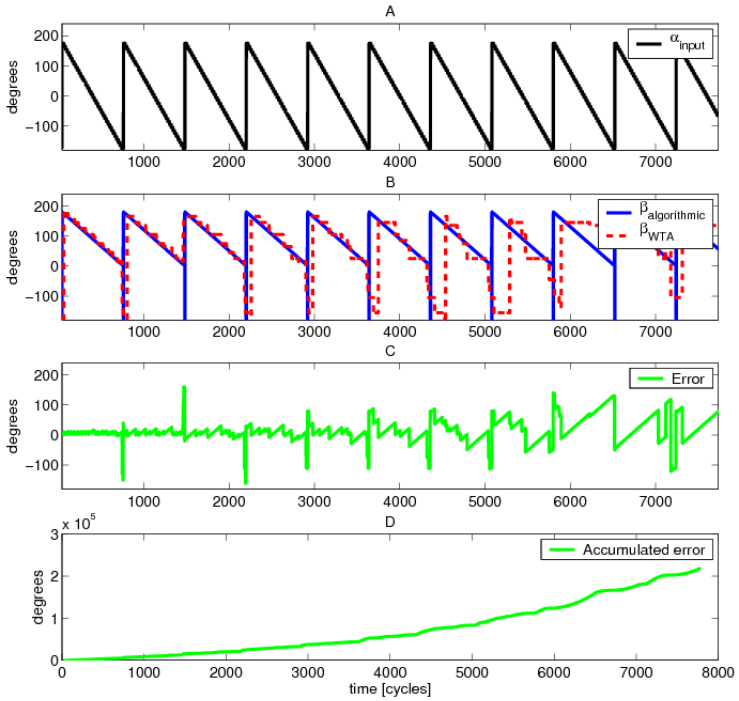

Figure 10 Quantification of an example of a simulation for the path memory system fed with data corresponding to a rotating turn table. A) α_{input} is the input angle feed into the model. The velocity was kept constant. B) β stands for the angle of the vector pointing to the assumed start location. β_{WTA}: β as computed by the neuronal memory readout mechanism based on the memory state, $\beta_{algorithmic}$: theoretical β computed algorithmically based on the input angle α and velocity v. C) Error indicates the angular difference between β_{WTA} and $\beta_{algorithmic}$ D) Accumulated angular difference over time

The first experiments performed consisted of feeding simulated direction information corresponding to information from a compass set on a rotating turn table into the path memory system (figure 10).

Data of this experiment shows that the accuracy of the system is high, and that the decay of accuracy starts only at ∼3800 time steps (figure 10B, C). The time course of the accumulated error (figure 10D), is nearly linear which means that the path information does not become abruptly unusable. The peaks in the angular deviation (figure 10C) can be attributed to a shift between the two angles over time.

3.2 Simulations based on paths of tracked ants

In a second set of experiments we applied the path memory model to 34 traces of ants exploring a novel environment. The arenas the ants explored where of about 70x30cm, and consisted of 3 consecutive compartments. The three compartments were interconnected by means of small apertures in the midline. About 10 landmarks were placed in each compartment to prevent the ant from seeing the entry to the next compartment and make the foraging task more difficult. Ants were individually marked, and the foraging data corresponds to 17 ants that were tracked during their first, second and third outbound journeys.

Based on the tracking data provided by AnTS – position of the ant over time – we calculated heading direction and speed of the ant. Subsequently heading direction and speed were fed into the path memory system via the groups "*heading*" and "*velocity*" (figure 4).

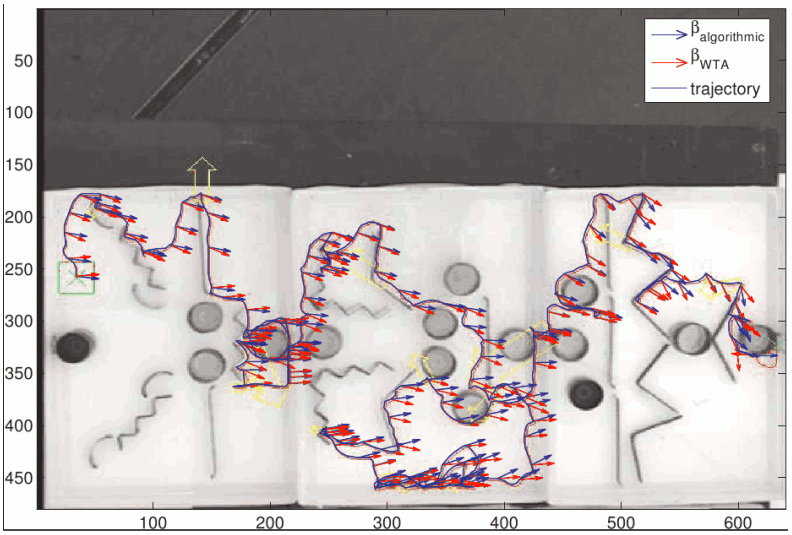

Figure 11 Example of path memory model applied to an ant trace. The trajectory start at the right side with the ant entering the arena, and ends at the left side with the ant reaching the food source. Blue arrows indicate the angle of the vector pointing to the assumed start location computed algorithmically based on the input angle, red arrows point to the start location as computed by the path memory system. The landmarks in the arena consisted of plastic cylinders and bent profiles of a height of ∼5cm.

An example of a trajectory of a tracked ant (figure 11) shows that the path consists of straight and convoluted sections. The plot of the orientation of the ant against time (figure 12A) shows that the ant was changing its heading direction frequently, with turn of up to 180°. The green arrows overlaid over the trajectory indicate the direction to the start location as computed by the path memory system. These arrows show that during the first period, the angle was not memorized correctly, but recovered towards the end of the path. This observation is confirmed if the angular deviation is plotted against time (figure 12B, C). Similarly to the results obtained from the turn table experiments, the accumulated error is nearly linear (figure 12D).

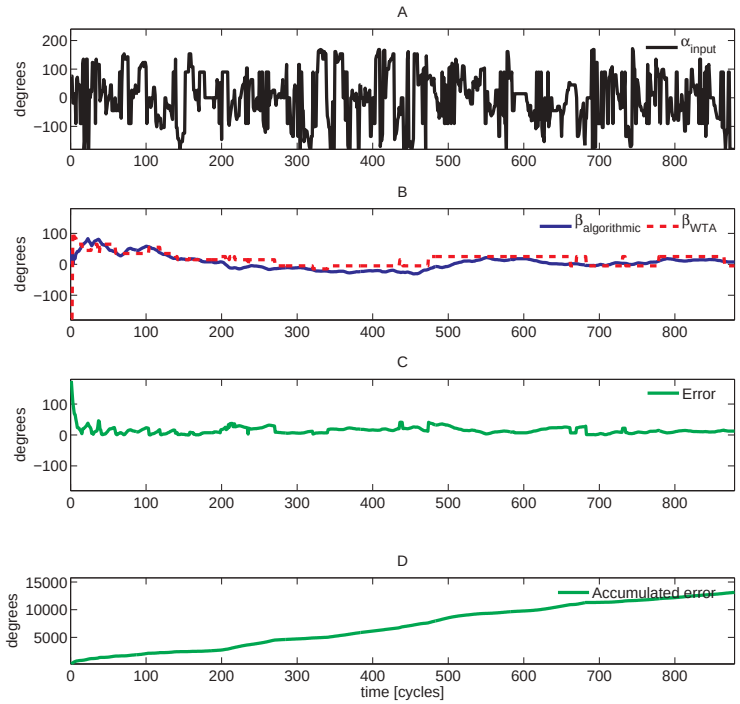

Figure 12 Quantification of an example of the path memory model applied to an ant trace. The input angle α_{input}, and the speed were reconstructed based on the recorded coordinates of the animal. A) α_{input} is the angle of the input. The velocity was kept constant. B) β stands for the angle of the vector pointing to the assumed start location. β_{WTA}: β as computed by the neuronal memory readout mechanism based on the memory contents, $\beta_{algorithmic}$: theoretical β computed algorithmically based on the input angle α and velocity v. C) Error indicates the angular difference between β_{WTA} and $\beta_{algorithmic}$ D) Accumulated angular difference over time.

To systematically quantify the behavior of our model, we computed the average performance of the system over 34 ant traces (figure 13). The traces stem from different animals, and different arrangements of the experimental arena, and the length of the traces varied up to a factor of 16.

The mean angular deviation was $\sim 20°$(figure 13a). The plot of the mean angular deviation against time (figure 13a), confirms that the system is not performing well at computing the angle at the start of the trajectory, but needs about $\sim$100 time steps before the angular deviation decreases.

The histogram of the distribution of the angular deviation from the algorithmically computed vector pointing to the start location shows a peak at $\sim 20°$ deviation (figure 13b). No traces had an average angular deviation larger than 70°. For a majority of traces the accumulation of angular deviation flattens out over time (figure 13c), i.e. did not increase exponentially.

Next to the estimation of the direction to the point of departure, assessment of the distance travelled can be vital in dead reckoning. In our path memory model, the total distance travelled is represented by the number of active neurons in the *"Memory"* group. To quantify the performance of the model we compared the length of the ants'

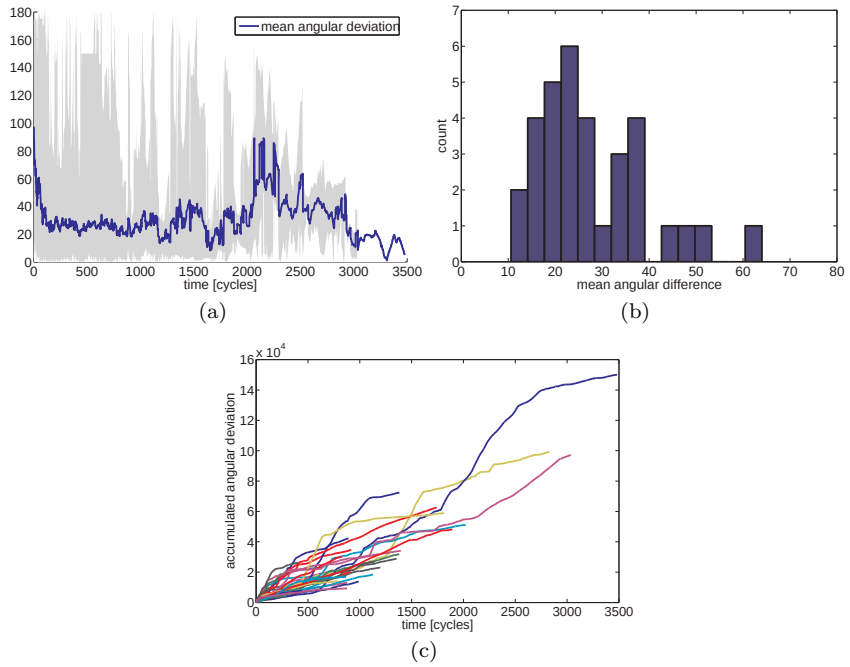

Figure 13 Quantification of the path memory model based on 34 ant traces. a) Angular deviation against time. Shaded areas indicate runs which yielded minimum, and maximum deviation, whereas the blue line indicates the mean. b) Histogram of the distribution of the average deviation over time. c)Deviation between β_{WTA} and $\beta_{algorithmic}$ accumulated over time. Each line stands for a single trace.

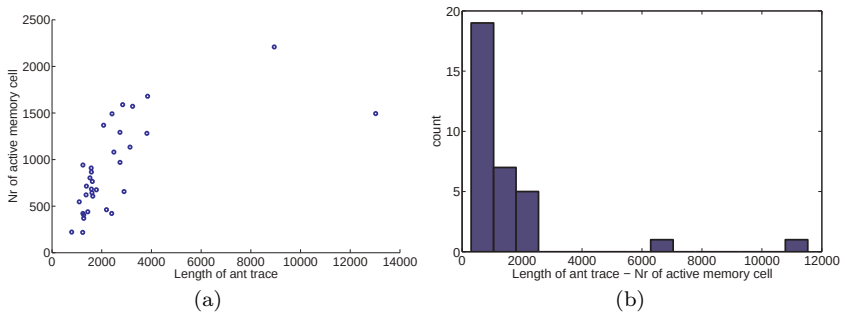

Figure 14 Quantification of the path length as estimated by the path memory model based on 34 ant traces. a) Scatter plot of the distance at the end position calculated from the ant traces vs. distance estimated by the path memory model represented by the number of active cells in the *"Memory"* group. b) Histogram of the difference between the travelled distance calculated from the ant traces and the estimate of the path memory model.

path the end point, calculated based on the tracking data, with the number of active cells in the *"Memory"* group (figure 14). The data shows that – except for two out-liners – the model can store information about the path length in a reliable fashion.

4 Discussion

Animals display amazing feats of exploration and homing, and an important questions is how the nervous systems of navigating animals like ants are solving this task in such an efficient way. We have presented a memory system for path integration that stores vectorial information and decodes the memory in a readout stage. Both the memory and the readout stage are based on the concept of the population code. Our model is biologically plausible in that it does not rely on neurons that perform trigonometric functions. Instead the required trigonometric operations are approximated in the specific connectivity between neurons, and the weights of the connections. The assumption made is that the synaptic weights between two groups of neurons are distributed in a Gaussian fashion. This conjecture seems by far more biologically plausible, than the assumption that single neurons are able to perform trigonometric operations. The memory of our model is based on a population of neurons which show persistent firing, and hence does neither depend on single a neuron nor on a neuron's capability to remain at a constant membrane potential over an extended period of time. Encoding vectorial information in a population code is a schema found in many neuronal structures. Yet it is still an open scientific question, how biological neuronal networks are decoding the population code. We built a circuit to readout the information stored in the population based on the spatial distribution of the connection weights, and a winner-take-all network.

We tested our model in two paradigms. First by reading direction information from a simulated compass, and secondly, by applying the model to data recorded from ants exploring a novel environment.

We were able to show that our path memory system was able to reliably store and compute the angle of the vector pointing to the start location, in both setups. Moreover we could show in the analysis of the simulation based on the ant traces, that the path memory system stores the total length of the trajectory in a dependable way.

It is not surprising to find a wealth of path integrating and landmark navigation systems in the field of robotics, as path integration would appear to be a fundamental requirement of a navigating real-world system [43]. Many of these systems are inspired by, but not grounded in biology (e.g. [33]). Conversely, neuron based models of path integration of varying biological plausibility [14,57,49], often lack embedding into a real-world artifact. Little work has been done until now combining plausible neuronal processing with a robotics approach [32]. However, the latter has a focus on occlusions, and does not implement a full behavioral cycle. One of the robotics approaches stand out by using a hardware realization of a celestial compass [23,22]. However, although the input stage is biologically plausible, the path integration and landmark navigation components themselves are realized in an algorithmic way irrespective of any biological constraints.

The major draw back of our model is that the direction information is stored in a discrete number of bins. This inherently restricts the accuracy of the computation of the homeward pointing angle. If it was possible to perform a vector decomposition at the input stage, it would be possible to use a memory group representing only three non-orthogonal directions, and yet store the angular information more precisely then possible in the present model. As with all models of path integration, the error is accumulating over time. Interestingly though, the results from the application of the model to the ant traces show that the error is not increasing monotonically, but tends to decrease over time.

"Consuming" memory In the path memory model presented here, the memory will fill up over time; once all the cells in a column are spiking, no more information can be stored. A system with "consuming" memory would be able to circumvent this. In this model the cells in a column corresponding to the current direction would only be excited, if the column at 180° offset had no cells spiking. If the column at 180° offset had active cells, this column would be inhibited, i.e. the number of spiking cells would be reduced (figure 15).

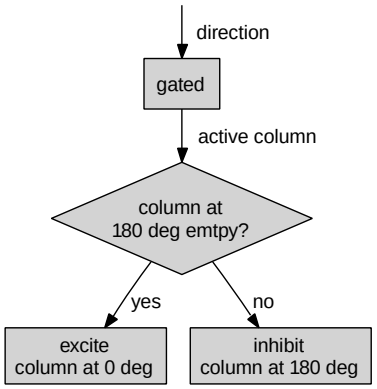

Figure 15 Abstract representation of the "consuming" memory mechanism. The length of the vector corresponding to the direction of the input is only increased, if the vector at 180° offset has a length of 0.

If the agent travels only in one single direction, the "consuming" model has obvious advantages with respect to the length of the path which can be stored. The advantages come to bear if the path includes directions which are 180° offset; in this case a much longer path can be stored. The downside being that the total length of the journey can not be calculated from the total number of the active cells, but only the sum of the vectors, which corresponds to the distance between the current position and the location of the point of departure. For most biological systems a rough estimate of the overall distance traveled will suffice. Support for this view comes from the behavior of bees; what they communicate to their hive mates in their "waggle dance" [50] is the air-line distance to the food source and not the distance they traveled in order to find the food source in the first place.

The performance, in terms of accuracy and update speed, of the path memory system makes the model suitable for application in the real-world, i.e. allows to embed the model in an agent behaving in the physical world in real-time. Firstly, this is important because the real-world applies very clear constraints at both the construction and evaluation level of a model, since the properties of the elements of the model have to obey the laws of physics in their construction as well as in the interaction with the real-world. Systems applied in the real-world can circumvent the typical problem of pure simulations of a low degree of generalizability.

Secondly, the real-world embedding is crucial because cognition and behavior are intricately linked, not allowing to separate them neatly into a cognitive and behavioral component [48]. In case of our model this can mean that the cognition does have repercussion on the behavior not only at the end of the travel in that it determines

where the agent assumes the starting location is, but also during the outbound journey, e.g. in that the memory fill state is continuously readout and will determine when the animal start the home bound travel. We can even go as far as speculating that the properties of the excursion path are in part defined by the memory mechanism; the agent would shape the trajectory not only to maximize the chance to find e.g. a food source, but also choose a path which can be stored well in memory.

Based on our simulation data, we predict there is a correlation between the number of cues in an environment and the path length in that foraging insects would have a minimal distance they travel in an environment without landmarks, as short distances are more prone to error in the calculation of the homeward pointing vector. On the neurobiological level we predict that the ant brain employs a population code like mechanism to store the essentially vectorial information required to integrate the path information over time. From the comparison of the two variations of the path memory models presented here, we derive the prediction that the "consuming" memory should be more suitable in describing the biological system. If the "consuming" memory mechanism hypothesis holds true, the memory should saturate slower if the path is random, but faster if the path non random. On the neurobiological level this prediction can be assessed by measuring the number of persistently firing neurons. We are evaluating these predictions in current experiments.

Acknowledgements The authors thank Dr Markus Knaden for providing them with the behavioral data of the ants.
This project was supported through the EU Future and Emerging Technologies program (IST-2001-33066-AMOTH).

References

1. Angstadt, J.: Persistent inward currents in cultured Retzius cells of the medicinal leech. J Comp Physiol [A] **184**, 49–61 (1999)
2. Bernardet, U.: iqr – large-scale neural systems simulator (2007). *http://iqr.sourceforge.net*
3. Bernardet, U., Blanchard, M., Verschure, P.: Iqr: a distributed system for real-time real-world neuronal simulation. Neurocomputing **44-46**, 1043–1048 (2002)
4. Darwin, C.: Origin of Certain Instincts. Nature **7**, 417–418 (1873)
5. Egorov, A., Hamam, B., Fransén, E., Hasselmo, M., Alonso, A.: Graded persistent activity in entorhinal cortex neurons. Nature **420**, 173–8 (2002)
6. Elias, S., Grossberg, S.: Pattern formation, contrast control and oscillations in the short term memory of shunting on-center off-surround networks. Biological Cybernetics (20), 69–98 (1975)
7. Esch, H., Burns, J.: Distance estimation by foraging honeybees. J Exp Biol **199**, 155–62 (1996)
8. Etienne, A., Jeffery, K.: Path integration in mammals. Hippocampus **14**, 180–92 (2004)
9. Feldman, J., Ballard, D.: Connectionist models and their properties. Cognitive Science **6**, 205–254 (1982)
10. Fukushima, K.: Neocognitron: a self organizing neural network model for a mechanism of pattern recognition unaffected by shift in position. Biol Cybern **36**(4), 193–202 (1980). 0340-1200 (Print) Journal Article
11. Gabbiani, F., Krapp, H., Koch, C., Laurent, G.: Multiplicative computation in a visual neuron sensitive to looming. Nature **420**, 320–4 (2002)
12. Georgopoulos, A.: New concepts in generation of movement. Neuron **13**, 257–68 (1994)
13. Georgopoulos, A., Schwartz, A., Kettner, R.: Neuronal population coding of movement direction. Science **233**, 1416–9 (1986)
14. Hartmann, G., Wehner, R.: The ant's path integration system: a neural architecture. Biol Cybern **73**, 483–497 (1995)

15. Hertz, J., Krogh, A., Palmer, R.: Introduction to the Theory of Neural Computation. Addison-Wesley Publishing Company, Redwood City, CA (1991)
16. Homberg, U., Würden, S.: Movement-sensitive, polarization-sensitive, and light-sensitive neurons of the medulla and accessory medulla of the locust, Schistocerca gregaria. J Comp Neurol **386**, 329–46 (1997)
17. Hrncir, M., Jarau, S., Zucchi, R., Barth, F.: A stingless bee (Melipona seminigra) uses optic flow to estimate flight distances. J Comp Physiol A Neuroethol Sens Neural Behav Physiol **189**, 761–8 (2003)
18. Jacobs, G., Theunissen, F.: Functional organization of a neural map in the cricket cercal sensory system. J Neurosci **16**, 769–84 (1996)
19. Knierim, J., Kudrimoti, H., McNaughton, B.: Place cells, head direction cells, and the learning of landmark stability. . J Neurosci **15**, 1648–59 (1995)
20. Labhart, T.: Polarization-opponent interneurones in the insect visual system. Nature **331**, 435–437 (1988)
21. Labhart, T., Meyer, E.P., Schenker, L.: Specialized ommatidia for polarization vision in the compound eye of cockchafers, *Melolontha melolontha* (coleoptera, scarabaeidae). Cell and Tissue Research **268**(3), 419–429 (1992)
22. Lambrinos, D.: Navigation in desert ants: the robotic solution. Robotica **21**, 407–426 (2003)
23. Lambrinos, D., Möller, R., Labhart, T., Pfeifer, R., Wehner, R.: A mobile robot employing insect strategies for navigation. Robotics and Autonomous Systems **30**, 39–64 (2000)
24. Lewis, J., Kristan, W.: A neuronal network for computing population vectors in the leech. Nature **391**, 76–9 (1998)
25. Liu, G., Seiler, H., Wen, A., Zars, T., Ito, K., Wolf, R., Heisenberg, M., Liu, L.: Distinct memory traces for two visual features in the Drosophila brain. Nature **439**, 551–6 (2006)
26. Loesel, R., Homberg, U.: Anatomy and physiology of neurons with processes in the accessory medulla of the cockroach Leucophaea maderae. J Comp Neurol **439**, 193–207 (2001)
27. Major, G., Tank, D.: Persistent neural activity: prevalence and mechanisms. Curr Opin Neurobiol **14**, 675–84 (2004)
28. Marr, D., Poggio, T.: A computational theory of human stereo vision. Proc R Soc Lond B Biol Sci **204**(1156), 301–28 (1979). 0080-4649 (Print) Journal Article
29. Menzel, R., Greggers, U., Smith, A., Berger, S., Brandt, R., Brunke, S., Bundrock, G., Hülse, S., Plümpe, T., Schaupp, F., Schüttler, E., Stach, S., Stindt, J., Stollhoff, N., Watzl, S.: Honey bees navigate according to a map-like spatial memory. Proc Natl Acad Sci U S A **102**, 3040–5 (2005)
30. Mercer, A., Kloppenburg, P., Hildebrand, J.: Plateau potentials in developing antennal-lobe neurons of the moth, Manduca sexta. J Neurophysiol **93**, 1949–58 (2005)
31. Mittelstaedt, M.L., Mittelstaedt, H.: Homing by Path Integration in a Mammal. Naturwissenschaften **67**, 566–567 (1980)
32. Mudra, R., Douglas, R.: Self-correction mechanism for path integration in a modular navigation system on the basis of an egocentric spatial map. Neural Netw **16**, 1373–88 (2003)
33. Möller, R.: Insect visual homing strategies in a robot with analog processing. Biol Cybern **83**, 231–243 (2000)
34. Pascual, A., Préat, T.: Localization of long-term memory within the Drosophila mushroom body. Science **294**, 1115–7 (2001)
35. Ramirez, J., Pearson, K.: Octopamine induces bursting and plateau potentials in insect neurones. Brain Res **549**, 332–7 (1991)
36. Reinhard, J., Srinivasan, M., Zhang, S.: Complex memories in honeybees: can there be more than two? J Comp Physiol A Neuroethol Sens Neural Behav Physiol **192**, 409–16 (2006)
37. Reppert, S., Zhu, H., White, R.: Polarized light helps monarch butterflies navigate. Curr Biol **14**, 155–8 (2004)
38. Ronacher, B., Gallizzi, K., Wohlgemuth, S., Wehner, R.: Lateral optic flow does not influence distance estimation in the desert ant Cataglyphis fortis. J Exp Biol **203**, 1113–21 (2000)
39. Rossel, S., Wehner, R.: Polarized vision in Bees. Nature **323**, 128–131 (1986)
40. Salinas, E., Abbott, L.: Vector reconstruction from firing rates. J Comput Neurosci **1**, 89–107 (1994)

41. Si, A., Srinivasan, M., Zhang, S.: Honeybee navigation: properties of the visually driven 'odometer'. J Exp Biol **206**, 1265–73 (2003)
42. Sommer, S., Wehner, R.: The ant's estimation of distance travelled: experiments with desert ants, Cataglyphis fortis. J Comp Physiol A Neuroethol Sens Neural Behav Physiol **190**, 1–6 (2004)
43. Spero, D.: A review of outdoor robotics research. Tech. Rep. MECSE-17-2004, Department of Electrical and Computer Systems Engineering, Monash University, Melbourne, Australia (2004). URL citeseer.ist.psu.edu/spero04review.html
44. Srinivasan, M., Zhang, S., Altwein, M., Tautz, J.: Honeybee navigation: nature and calibration of the "odometer". Science **287**, 851–3 (2000)
45. Stalleicken, J., Mukhida, M., Labhart, T., Wehner, R., Frost, B., Mouritsen, H.: Do monarch butterflies use polarized skylight for migratory orientation? J Exp Biol **208**, 2399–408 (2005)
46. Taube, J.: The Head Direction Signal: Origins and Sensory-Motor Integration. . Annu Rev Neurosci pp. – (2007)
47. Tautz, J., Zhang, S., Spaethe, J., Brockmann, A., Si, A., Srinivasan, M.: Honeybee odometry: performance in varying natural terrain. PLoS Biol **2**, – (2004)
48. Verschure, P., Voegtlin, T., Douglas, R.: Environmentally mediated synergy between perception and behaviour in mobile robots. . Nature **425**, 620–624 (2003)
49. Vickerstaff, R., Di Paolo, E.: Evolving neural models of path integration. J Exp Biol **208**, 3349–66 (2005)
50. von Frisch, K.: The Dance Language and Orientation of Bees. Harvard University Press, Cambridge (1993)
51. von Philipsborn, A., Labhart, T.: A behavioural study of polarization vision in the fly, musca domestica. Journal of Comparative Physiology A: Neuroethology, Sensory, Neural, and Behavioral Physiology **167**(6), 737–743 (1990)
52. Wallace, D., Hines, D., Pellis, S., Whishaw, I.: Vestibular information is required for dead reckoning in the rat. J Neurosci **22**, 10,009–17 (2002)
53. Wehner, R.: Orientation and communication in arthropodes, chap. The ant's celestial compass system: spectral and polarization channels, pp. 145–185. Birkhäuser, Basel (1997)
54. Wehner, R.: Desert ant navigation: how miniature brains solve complex tasks. J Comp Physiol A Neuroethol Sens Neural Behav Physiol **189**, 579–88 (2003)
55. Wehner, R., Srinivasan, M.: The Neurobiology of Spatial Behaviour, chap. Path integration in insects, pp. 9–30. Oxford University Press (2003)
56. Wittlinger, M., Wehner, R., Wolf, H.: The ant odometer: stepping on stilts and stumps. Science **312**, 1965–7 (2006)
57. Wittmann, T., Schwegler, H.: Path integration - a network model. Biological Cybernetics **73**(6), 569–575 (1995). DOI 10.1007/s004220050212
58. Wohlgemuth, S., Ronacher, B., Wehner, R.: Ant odometry in the third dimension. Nature **411**, 795–8 (2001)
59. Yu, A., Giese, M., Poggio, T.: Biophysically plusible implementations of the maximum operation. Neural Computation **14**, 2857–2888 (2002)
60. Yuille, A., Grzywacz, N.: A computational theory for the perception of coherent visual motion. Nature **333**(6168), 71–74 (1988). 0028-0836 (Print) Journal Article
61. Zars, T., Fischer, M., Schulz, R., Heisenberg, M.: Localization of a short-term memory in Drosophila. Science **288**, 672–5 (2000)
62. Zars, T., Wolf, R., Davis, R., Heisenberg, M.: Tissue-specific expression of a type I adenylyl cyclase rescues the rutabaga mutant memory defect: in search of the engram. Learn Mem **7**, 18–31 (2000)
63. Zhang, S., Bock, F., Si, A., Tautz, J., Srinivasan, M.: Visual working memory in decision making by honey bees. Proc Natl Acad Sci U S A **102**, 5250–5 (2005)